Arching around buried square section structures

Arquer autour des structures de section de carré enterrées

O.S. Abuhajar, T. Newson & M.H. El Naggar
Geotechnical Research Centre, University of Western Ontario, Canada.
K. Stone
Department of Civil Engineering, University of Brighton, United Kingdom.

ABSTRACT
It is recognized that the loads attracted to buried structures cannot be accurately estimated by simply considering the self-weight forces generated by the prism of soil supported by the structure. Incompatibility between the stiffness of a buried structure and the surrounding soil leads to the development of local soil arching around the structure, the degree of which is dependent on the relative stiffness between the structure and the surrounding soil. This arching can induce structural damage or collapse, or indeed can be utilized to optimize the efficiency of the structure. The paper presents numerical finite element analysis of the results of a series of scaled physical model tests conducted on a large fixed beam centrifuge designed to investigate the contribution of the deflection of structural elements (top slab and side wall) of a buried structure and local soil stiffness, to the overall loads attracted to the structure. The results of the test program have been interpreted to establish the contributions to the total load attracted to a buried structure from deflection of the top slab and the side-walls respectively. Results of comparative analyses using the finite element software Plaxis are presented.

RÉSUMÉ
Il est reconnu que les chargements attirés aux structures enterrées ne peuvent pas être précisément estimés par considérant simplement le pèse automatiquement des forces produites par le prisme de sol soutenu par la structure. L'incompatibilité entre la raideur d'une structure enterrée et le sol environnant mene au développement d'arquer de sol local autour de la structure, le degré que dont dépend de la raideur relative entre la structure et le sol environnant. Cet arquer peut induire des dommages ou l'effondrement structurels, ou peut être utilisé en effet pour optimiser l'efficacité de la structure. Le papier présente les résultats d'une collection des tests modèles, physiques et gradué dirigés sur un grand centrifugeur de rayon fixe ont conçu pour examiner la contribution de la déflexion d'éléments structurels (la premiers dalle et le mur de côté) d'une structure enterrée et de raideur de sol locale, aux chargements généraux attirés à la structure. Les tests utilisent des buses modèles d'une section carrée uniforme. La tension jauge adhéré aux buses modèles permet une mesure directe de courber de moments et donc les chargements être obtenus pendant le test de centrifugeur. Les résultats du programme de test ont été interprétés pour établir les contributions au chargement total attiré à une structure enterrée de la déflexion de la première dalle et la paroi respectivement. Les résultats de comparatif analysent utilisant l'élément fini Plaxis de logiciel est présenté.

Keywords : soil-structure interaction, stiffness, arching, culvert, centrifuge, finite element.

1. INTRODUCTION

The loads attracted to buried structures, from both overburden and surcharge loads, are governed by the characteristics of soil and the geometry and stiffness of the structural components. In many instances, the redistribution of free-field stresses as the result of the presence of a buried structure will result in a decrease in loading over the deflecting or yielding areas of the structure and an increase over adjoining rigid or stationary parts. This transfer of load due to soil-structure interaction is known as 'arching'.

Whilst there have been experimental and field studies to investigate stress distribution and arching (e.g. Lefebvre et al., 1976), the exact conditions required for this phenomenon to occur are still unclear and arching is often ignored in engineering design due to a lack of experience, and inclusion in codes of practice is rare. A range of problems such as underground conduits, tunnels, trapdoors, retaining walls and braced cuts can all experience significant arching action and theoretical analyses have been published on these subjects. These approaches have considered soil arching from both elastic and plastic soil states. Iglesia et al. (1999) presented a model for estimation of loads on underground structures based on the ground reaction curve. More recently, arching around buried structures has been studied in centrifuge model tests (e.g. Iglesia et al., 1999; Stone & Newson, 2002).

1.1 *Rectangular buried structures*

Buried culverts and conduits are commonly used around transportation infrastructure, e.g. to span highways. These are used to control water flow, storm runoff, divert municipal services, allow vehicular access and for other related activities. The geometry of these structures is usually circular or rectangular in cross-section and can have single or multi-celled openings. In recent years research has concentrated on the behaviour of flexible circular culverts and large diameter pipelines. However, knowledge of arching around rectangular and square culverts is currently limited. Numerical study of negative and positive arching around deeply buried rigid box culverts was conducted by Kim and Yoo (2005), with emphasis on the imperfect trench method of construction. The current edition of the AASHTO (2002) standard specifications for highway bridges takes some account of arching by changing vertical stresses over box culverts based on Marston-Spangler theory. However, this approach is quite conservative compared to more sophisticated numerical techniques, such as finite element analysis.

For the case of relatively flexible buried structures, the soil-structure interaction is even more complicated and the problem is difficult to solve theoretically or analytically. However, it is relatively simple to examine the problem experimentally and in particular with a geotechnical centrifuge. Some of the results of

Proceedings of the 17th International Conference on Soil Mechanics and Geotechnical Engineering
M. Hamza et al. (Eds.)

doi:10.3233/978-1-60750-031-5-3408

a geotechnical centrifuge study completed by the authors with this aim have already been reported (e.g. Stone and Newson, 2002). The principal aim of this particular paper is to report part of the interpretation of these experimental tests, using finite element analysis and this has enabled comparison of the contribution made by the structural elements (i.e. sidewalls, top and base slabs) to the loads attracted to the structure, in comparison to theoretical overburden loads. In the interests of brevity, only the numerical analysis will be shown in this paper, although a description of aspects of the numerical testing will be described to provide a better understanding of the rationale for the numerical analysis for the reader.

2 EXPERIMENTAL METHOD

2.1 *Model box culvert*

In general, box culverts are constructed from short sections of reinforced concrete, which are joined together to form the final desired cross-section. Due to the problems of manufacturing concrete with micro-aggregates for scaled model testing, the model culvert (shown in Figure 1) was made from an aluminum box section with an original external dimension of 101.6 mm (i.e. width, B and height, H are equal) and an initial wall thickness of 6.35 mm.

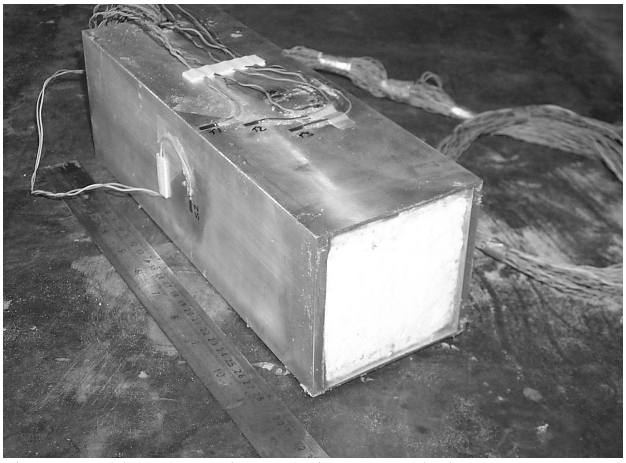

Figure 1. Model culvert prior to placing on sand bed.

However, correct modeling of the structural deflection can be achieved in reduced scale models by ensuring the following relationship is maintained:

$$E_m/I_m = E_p/I_p/N^4 \quad (1)$$

where, E = Young's modulus of the material, I = second moment of area per unit length of the material and N = scaling factor. The subscripts 'm' and 'p' refer to model and prototype respectively.

To improve the response of the model, the walls of the aluminum section were machined to a thickness of 2 mm. Miniature strain gauges were bonded at various locations on culvert to record internal and external strains. The outputs were used to determine bending and axial strains at the location of each gauge pair.

2.2 *Centrifuge tests*

The centrifuge test procedure was as follows: firstly a bed of sand was placed by pluviation through air into a rectangular strongbox of dimensions 500 mm wide x 800 mm long x 600 mm high. The strongbox was then mounted on the centrifuge platform and the culvert placed on this layer. The strain gauges were connected to the data acquisition system, and after checking their initial gauge output, the data logger was zeroed. The centrifuge was then accelerated and held at the following acceleration levels, 5g, 10g, 20g, 40g, 60g and 80g. Data from the strain gauges was recorded continuously during the test. Congleton Sand was used for all the tests. This is a uniform sand with a d_{10} = 100 μm and maximum and minimum densities of 1.78 and 1.51 g/cm^3 respectively. The angle of internal friction at critical state is ϕ' =31°. In this paper, two of the culvert orientations are presented, one of them is the typical parallel position and the other rotated to 45° as shown in Figure 2 below.

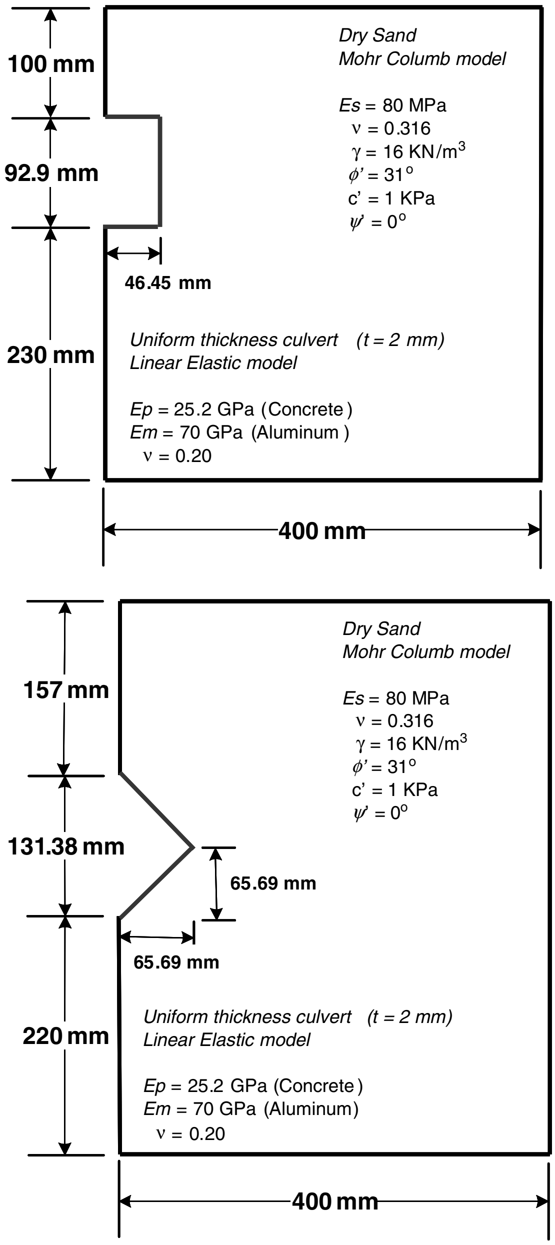

Figure 2. Schematic diagram showing the orientation of the two culverts and the properties used for analysis.

3 NUMERICAL MODELING

The first test refers to the case of a 100 mm model depth of soil overburden on a parallel culvert and the second test refers to the case of the culvert with the top slab rotated to 45^o with horizontal as shown in Figure 2. Both culverts were uniform in thickness (2 mm) and the tests were run up to the 80g-level with increments of 5, 10, 20, 40, 60 and 80g (i.e. the scaling factor N). The numerical analysis results presented herein are for the level of 20g test only. These tests were designed to investigate the interaction between the buried model and the surrounding soil as a function of the stiffness of the soil and deformation of the model, which will be discussed in terms of the numerical analysis.

Two dimensional plane strain finite element analysis of the centrifuge test was conducted using the package PLAXIS® to aid interpretation of the physical model. Drained soil conditions were assumed and the modeling was carried out using Mohr-Coulomb elastic-perfectly plastic soil. The assumed material parameters were Young's modulus, E = 80 MPa, Poisson's ratio, $\nu' = 0.32$, effective unit weight, $\gamma = 16$ kN/m^3 (note the sand was dry), angle of internal friction, $\phi' = 31^\circ$, cohesion angle, $c' = 1.0$ kPa and angle of dilation, $\psi' = 0^\circ$. The culvert material (assumed to be linear elastic) was assigned E = 70 GPa for aluminum and $\nu = 0.20$.

Due to symmetry, only the right side of the soil-structure system was modeled. The domain was discretized using 15-noded triangular soil elements (with fourth order interpolation for displacements) and 5-noded beam culvert elements. Each node has three degrees of freedom per node: two translational and one rotational. Interface elements were used to provide for possible slippage and separation between the culvert and the surrounding soil. In Plaxis, the 'roughness' of the interaction is defined by a strength reduction factor, R, which relates the interface strength to the soil strength parameters. A 33% reduction in soil strength was assumed (R = 0.67) at the interface between the culvert and the surrounding soil.

The geometry and finite element mesh used for both culverts are shown in Figure 3. There is a line of symmetry along the centre of the culvert. The boundary conditions used was to be fixed in horizontal direction for the sides and fixed in both direction in the bottom and free at the surface as shown in Figure 3. Figure 3 show also the deformed mesh and deflection in the culvert sides.

The total culvert displacement is shown in Figure 4 for both culverts; for each case, the maximum displacement is close to the mid span on both the top slab and side walls. In the parallel culvert (#1), the values of the displacement in the side and base are low, in comparison to the top slab, whilst for the rotated culvert (#2) the same ratio between the top and side wall displacements is close to 50%.

Figure 5 shows the bending moment distribution for the parallel and the rotated culverts at 20g for the top slab and side wall. The highest bending moments occur in the centre and at the edges (corners) of the culvert. In the parallel culvert (#1), the bending moment at the mid span for top and base slabs is not similar. The bending moment in the base is uniform for more than half the span and its value is small compared to the bending moment at mid top span and at corners. In the rotated culvert (#2) the bending moment is larger at the side corner and decreases towards the upper and lower corners.

The loads attracted to the top slab of both culverts were calculated using the prism load of overburden pressure and the resulted load obtained from the finite element analysis. Both culverts show reduced loads attracted to the upper slabs of the structure (Table 1).

The shear strain contours are shown in Figure 6. These show very little strain localization along the top and side of the parallel culvert, with the majority of the strains occurring close to the corner of the top slab with the highest magnitudes of 0.024% strain. The rotated culvert shows two high shear strain localizations on both sides of the culvert with highest magnitude. The value of the strain is 0.008% which is interestingly very low compared to the parallel culvert.

Table 1. Summary of loading attracted to the top slab(s) of the culverts. (All loads in kN/m at 20g)

Culvert	w_{prism}	w_{plaxis}	w_{plaxis} / w_{prism}
Parallel	64	57.96	0.90
Rotated	200.2	74.4	0.37

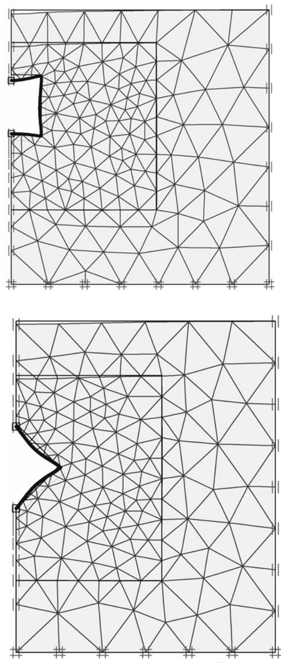

Figure 3. Geometry and finite element mesh for both culverts.

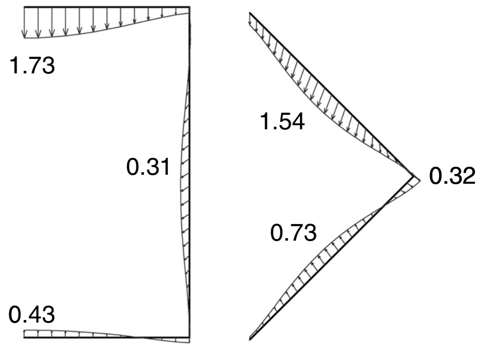

Figure 4. Total displacement diagrams for both culverts (m) (x10^{-3}).

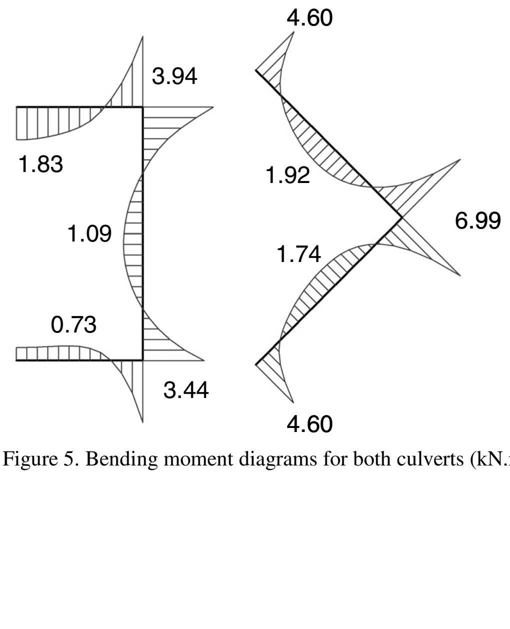

Figure 5. Bending moment diagrams for both culverts (kN.m/m)

The horizontal effective stress predicted using PLAXIS and acting on the side walls are shown in Figure 7 along with the loads predicted by assuming active, passive and *at-rest* pressure coefficients. These show that significant portions of the side walls are subjected to relatively low horizontal pressures; less than the active case in certain areas. The one exception is the corner of the rotated culvert, which has pressures that begin to approach the passive pressures.

For the parallel case (#1), the top slab is behaving in a similar manner to an active trapdoor (reducing the overall load attracted), whilst the side wall behaves like a propped wall. In the rotated case (#2), the two upper members again behave like an active trapdoor and the lower members like a propped wall. Both structures tend to reduce the total loads attracted to the top slabs, whilst concentrating the loads at the corners. For the rotated case, this behaviour is further enhanced by the additional compression of the upper members acting together (in a similar manner to a loaded 'A-frame' structure).

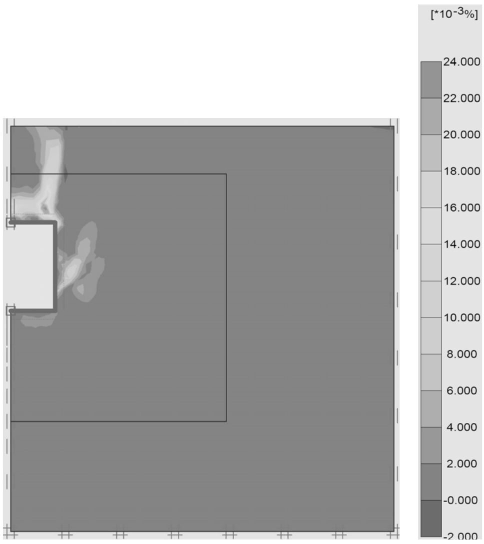

(a)

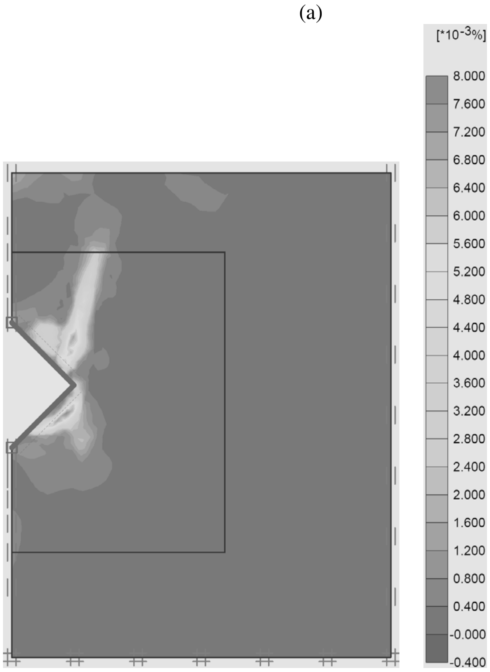

(b)

Figure 6. Contours of incremental shear strain: (a) parallel configuration; (b) 45° rotated configuration.

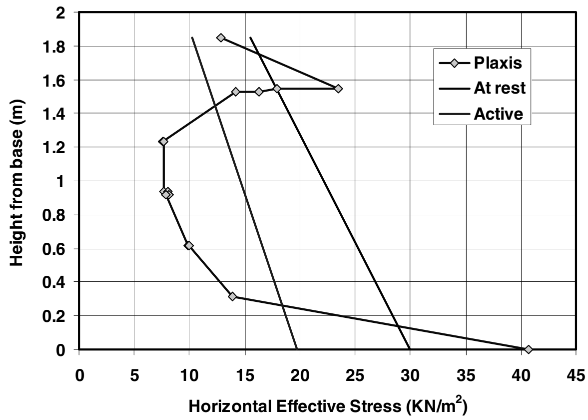

(a)

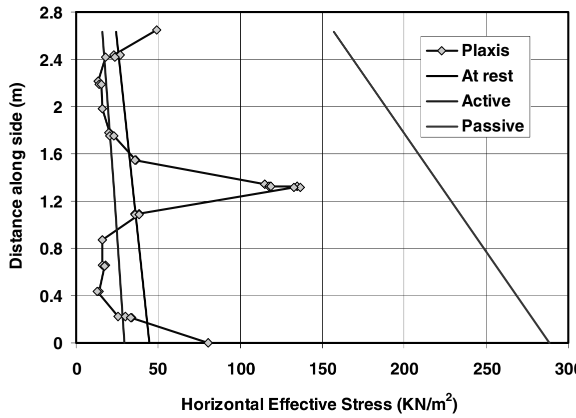

(b)

Figure 7. Horizontal soil pressure on side walls: (a) parallel configuration; (b) 45° rotated configuration.

4 CONCLUSIONS

This paper has describes numerical modeling of scaled models used to investigate a complex soil-structure interaction problem of a buried culvert. The analyses have investigated the contributions of the form and location of the structural elements to the load attracted to the top slab and side wall of the buried square box section. The results indicate that the deflection of the top slabs leads to active arching over the box culverts, reducing total loads and concentrating them at the corners of the structure. This suggests that control of the soil pressures around the structure can be achieved by varying the relative stiffness and orientation of the different structural members.

REFERENCES

American Association of State Highway and Transportation Officials, Inc. (AASHTO) 2002. *AASHTO Standard Specifications for Highway Bridges*, Washington, D.C.

Iglesia, G.R., Einstein, H.H., and Whitman, R.V. 1999. Determination of Vertical Loading on Underground Structures Based on an Arching Evolution Concept, *Geotechnical Special Publication*, 90: 495-506.

Kim, K. and Yoo, C.H. 2005. Design Loading on Deeply Buried Box Culverts, *J. of Geotech. & Geoenv. Eng. Div., ASCE*, 131(1): 20-27.

Lefebvre, G., Laliberte, M., Lefebvre, L.M., Lafleur, J. and Fisher, C.L. 1976. Measurement of Soil Arching above a Large Diameter Flexible Culvert, *Can. Geot. J.*, 13: 58-71.

Stone, K.J.L. and Newson, T.A. 2002. Arching Effects in Soil-Structure Interaction, *4th Int. Conf. Physical Modelling in Geomechanics*, St. Johns, Newfoundland, 935-939.